ELSEVIER

International Journal of Pharmaceutics 190 (1999) 1–11

international journal of pharmaceutics

www.elsevier.com/locate/ijpharm

Kinetics and mechanism of degradation of klerval, a pseudo-tetrapeptide

Chong Min Won *, Thomas E. Molnar, Vincent L. Windisch [1], Robert E. McKean

Department of Pharmaceutical Sciences, Rhone-Poulenc Rorer Research and Development, SW5, Collegeville, PA 19426-0107, USA

Received 12 April 1999; received in revised form 1 June 1999; accepted 2 June 1999

Abstract

The degradation of klerval (**I**) was studied as a function of pH. The extent and routes of degradation were found to be pH-dependent. Under strongly acidic conditions (pH < 2), the drug predominantly undergoes specific acid-catalyzed hydrolysis of the side-chain amide bond yielding **II**. In weakly acidic solutions (2 < pH < 4), the backbone amide bond was found to be hydrolyzed forming a tripeptide. The cleavage reaction proceeds via intramolecular catalysis by carboxyl group displacement of the nitrogen of the peptide bond. In addition, parallel formation of a small amount of succinimide was observed in acidic solutions (1 < pH < 5). In neutral solutions (5 < pH < 8), the peptide isomerizes via the succinimide producing the iso-aspartyl isomer. The isomerization was found to be pH-independent throughout neutral and basic pH regions. In basic solutions (pH > 8), the drug undergoes specific base-catalyzed hyrolysis yielding **II** and epimerization generating D-epimer. The epimerization appears to occur via the succinimide intermediate in neutral pH region. With increasing pH, however, the epimerization rate increases due to direct epimerization of the peptides.

Keywords: Klerval; Pseudo-tetrapeptide; Stability; Kinetics; Degradation; pH

1. Introduction

The binding of fibrinogen to an activated membrane-bound glycoprotein complex known as GPIIb/IIIa is the final obligatory step in platelet aggregation (Pytela et al., 1986). Arginine–glycine–aspartic acid (RGD) is an amino acid sequence in fibrinogen recognized by the platelet glycoprotein. Such binding ressults in the crosslinking of platelets by fibrinogen leading to aggregation and thrombus formation. Klerval (**I** in Scheme 1), *N*-ethyl-*N*-[1-oxo-4-(4-piperidinyl) butyl] glycyl-L-α-aspartyl-3-cyclohexyl-L-alaninamide, a pseudo-tetrapeptide and RGD peptidomimetics of platelet aggregation, is being developed for the prevention of arterial thrombus formation.

* Corresponding author. Tel.: +1-610-454-5170; fax: +1-610-454-2238.

E-mail address: chong.won@rp-rorer.com (C.M. Won)

[1] Present address: Absorption System, Exton, PA 19341, USA.

0378-5173/99/$ - see front matter

PII: S0378-5173(99)00195-7

The aspartyl residue on proteins and peptides has been reported to be potential degradation site (Piszkiewicz et al., 1970; Marcus, 1985; Geiger and Clarke, 1987; Kirsch et al., 1989; Stephenson and Clarke, 1989; Tsuda et al., 1990; Oliyai and Borchardt, 1993). Racemization and isomerization of the aspartyl residue as well as deamidation appear to be major degradation pathways in aspartyl peptides and proteins.

An understanding of the kinetics and mechanisms by which the drug degrades enables rational design of a suitable dosage form. The studies reported herein were undertaken to establish the pH effect on the rates of individual degradation routes and product distribution under both acidic and alkaline conditions. A separate experiment was performed to study the degradation of compound **II**.

2. Materials and methods

2.1. Materials

The purity of klerval (**I**) and **II** was greater than 99% as determined by high performance liquid chromatography (HPLC) analysis. HPLC grade acetonitrile and hexane sulfonic acid were used to prepare the mobile phase. Buffer reagents and all other chemicals were of reagent grade.

Hydrolysis fragments **III** and **IV** were prepared by degradation of **I** in aqueous acid. The cyclic imide (**V**) was prepared by non-aqueous degradation of **I** in DMF. The iso-peptide (**VI**) was prepared by aqueous degradation of **V** under basic conditions. The compounds were isolated by semi-preparative HPLC and the structures determined by FAB mass spectrometry and NMR. Other compounds were supplied by the Process Chemistry Department of Rhone-Poulenc Rorer Research and Development.

2.2. HPLC analysis

The HPLC system consisted of a pump (Hewlett Packard 1050), an autoinjector (Waters 710B), a UV detector (Hewlett Packard 1050), and a networking data acquisition system (Waters 860). The HPLC method employed a 150×4.6 mm i.d. 3 μm particle size, octadecyl-bonded silica-stationary-phase column (Keystone Hypersil BDS). The flow rate was 1.0 ml min^{-1} and the detector wavelength for UV absorbance detection was 210 nm. The column temperature was kept constant at 40°C. Separations were carried out as follows. An ion-pair buffer solution containing 40 mM NaH_2PO_4 and 10 mM hexane sulfonic acid in water, was prepared and the pH adjusted to 3.0 with H_3PO_4. Eluent A: ion-pair buffer solution/water (50:50); eluent B: ion-pair buffer solution/acetonitrile (50:50); 30 min linear gradient from 75% A (25% B) to 50% A (50% B); 20 min linear gradient from 50% A (50% B) to 0% A (100% B).

2.3. Kinetic methods

Stock solutions of **I** or **II** (1 mg ml^{-1}) and buffers (0.2 M) in water were prepared. An aliquot (2.5 ml) of the drug stock solution, an appropriate amount of hydrochloric acid (HCl) (pH 1.1–1.8), chloroacetate (pH 2.4–3.3), acetate (pH 4.0–5.8), phosphate (pH 6.8–7.8), borate (pH 8.4–9.0), or carbonate (pH 9.2–9.8) buffer stock solution and an appropriate amount of 1 M NaCl to maintain an ionic strength of 0.1 were transferred into a 25-ml volumetric flask and filled to volume with water. A low buffer concentration of 0.02 M was used to minimize possible general acid–base catalysis by the buffer species. The pH values of the buffer solutions were measured at the reaction temperature with a pH meter standardized at the same temperature. The pH values of HCl solutions at the reaction temperature were calculated using activity coefficients extrapolated from literature data (Harned and Owen, 1958). The reaction flask was kept in a constant-temperature water bath at 80.0°C (± 0.1). Samples were taken at appropriate time intervals and cooled to room temperature, and analyzed by HPLC using the method described previously.

2.4. Determination of rate constants

The dynamics of the degradation of **I, II** and the related compounds were described by differen-

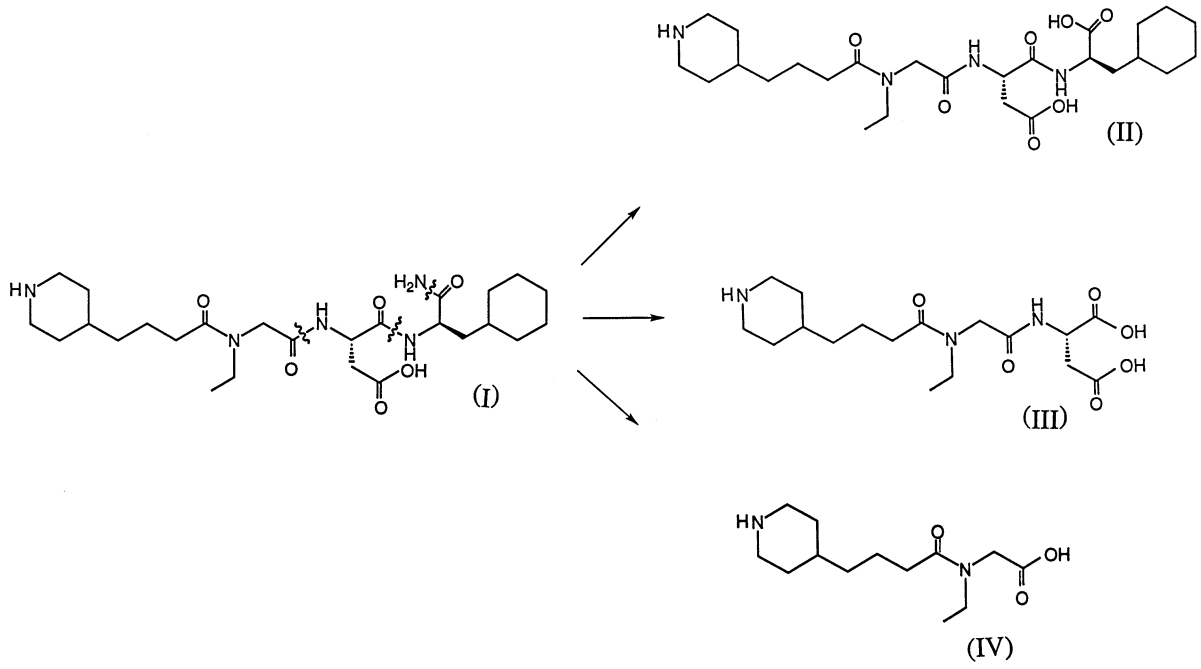

Scheme 1.

tial equations representing mass action terms and rate constants. The experimental data were fit using the integrated forms of the equations through nonlinear regression analysis. The curve-fitting was performed by a computer iteration procedure using RS/1 (BBN Software Products) or SigmaPlot (SPSS).

2.5. Determination of ionization constants

The ionization constants of **I** and **II** were determined by potentiometric titration using a Sirius PCA microtitrator (East Sussex, UK). To a 10 ml of 0.1 M KNO_3 solution containing 1 mg of **I** or **II**, 0.3 ml of 0.5M HCl was added to lower the pH to 2. The solution was titrated with 0.5 M KOH to pH 11. Titrated values for the side chain of aspartic acid (pK_{a1}) and piperidinyl ring (pK_{a2}) of **I** were 3.8 and 11.3, respectively. The pK_a values for the C-terminal caboxylic acid (pK_{a1}), the side chain of aspartic acid (pK_{a2}) and piperidinyl ring (pK_{a3}) of **II** were 3.0, 4.3 and 11.3, respectively.

3. Results and discussion

3.1. Product distribution

HPLC chromatograms showing the separation of the degradation products are given in Fig. 1. A total of three hydrolysis products (**II**, **III** and **IV**) have been observed in the degradation of **I** in aqueous solutions of various pH values. In addition to the cleavage products, L-succinimde (**V**), L-isoaspartyl isomer (**VI**), D-aspartyl epimer (**VII**), D-succinimide (**VIII**) and D-isoaspartyl isomer (**IX**) have been detected. The identification of the products was achieved by co-injecting authentic samples of the degradation products. The peak area mass balance of the reaction products was found to be 97–102% under most conditions studied.

3.2. Rate-pH profile

The kinetics of klerval degradation is affected by the ionization of the carboxylic acid (pK_{a1} = 3.8) of the aspartyl residue. However, the kinetics

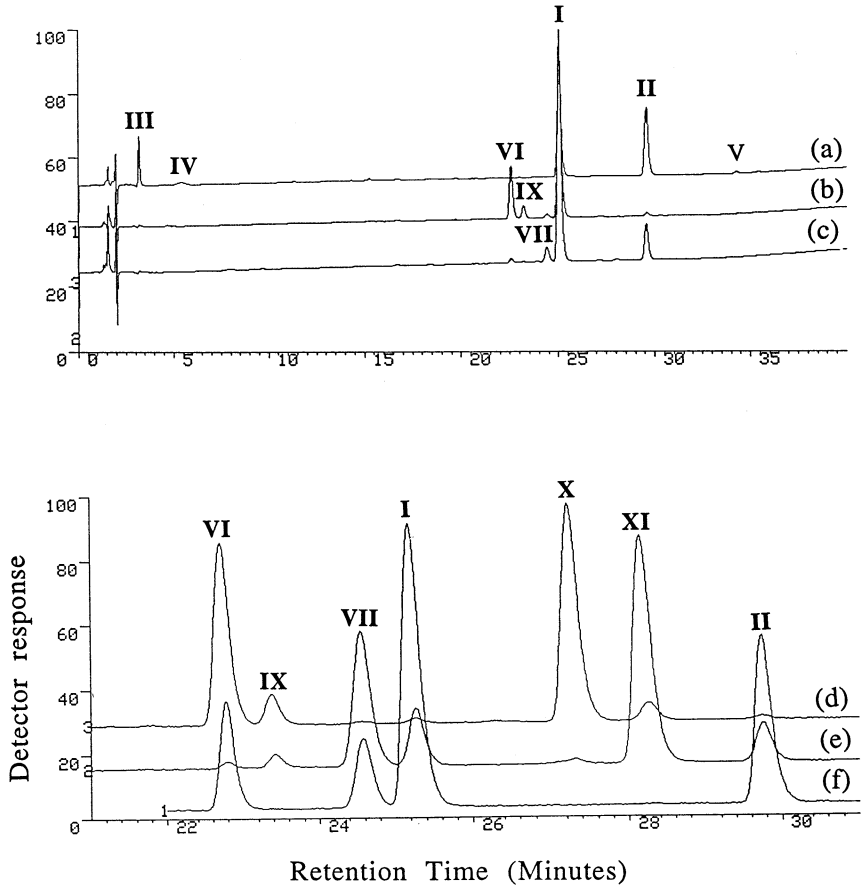

Fig. 1. High performance liquid chromatography (HPLC) chromatograms of degraded **I** (a, b, c) and related compounds (d, e) at 80°C in aqueous solutions. **X**, Deamidation product of **VI**; **XI**, deamidation product of **VII**. (a) pH 1.1, 3.5 h; (b) pH 7.0, 120 h; (c) pH 9.3, 8 h; (d) **VI**, pH 9.3, 50 h; (e) **VII**, pH 9.3, 50 h; (f) mixture of **I**, **II**, **VI** and **VII**.

is not affected by the secondary amine in the piperidinyl group ($pK_{a2} = 11.3$) because the pK_{a2} lies outside of the pH range studied. Below pH 3, **I** exists mainly in cationic form (A_c); between pH 4 and 10 in zwitterion (A_z); and above pH 10 in anion.

Although other kinetically equivalent reactions are not ruled out, the shape of the rate-pH profile indicates the occurrence of a specific acid-catalyzed process for the cation below pH 2 (k_H), water-catalyzed or spontaneous processes for the cation between pH 2 and 5 (k_o) and the zwitterion between pH 5 and 9 (k'_o), and a specific base-catalyzed process for the zwitterion above pH 9 (k'_{OH}). The rate expression for the kinetic scheme is:

$$\text{Rate} = k_{obs}[A] \quad (1)$$

where k_{obs} is the observed first-order rate constant and [A] is the total drug concentration. Since

$$[A] = [A_c] + [A_z] \quad (2)$$

where $[A_c]$ and $[A_z]$ are the concentrations of the cation and zwitterion, respectively. The observed rate constant (k_{obs}) can be formulated as:

$$\begin{aligned} k_{obs} &= (k_H[H^+] + k_o)f_c + (k'_o + k'_{OH}[OH^-])f_z \\ &= \{(k_H[H^+] + k_o)[H^+] \\ &\quad + (k'_o + k'_{OH}K_w/[H^+])K_{a1}\}/(K_{a1} + [H^+]) \end{aligned} \quad (3)$$

where f_c and f_z are the fractions of A_c and A_z, respectively.

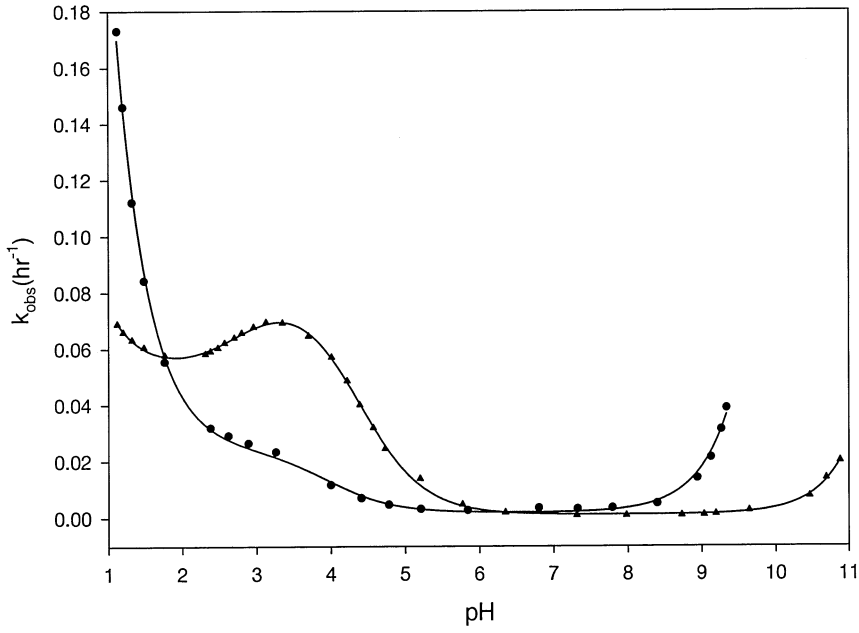

Fig. 2. The rate-pH profiles for the degradation of **I** (●) and **II** (▲) in aqueous solutions at 80°C. Ionic strength, 0.1. The solid lines are computer-generated curves based on Eqs. (3) and (4) and using obtained kinetic parameters in Table 1.

The experimental rate constants were fit to Eq. (3) using nonlinear regression analysis (Fig. 2). The rate constants and the pK_{a1} value obtained from the plot are given in Table 1. The solid line in Fig. 2 represents the theoretical curve calculated by substituting the rate constants in Table 1 into Eq. (3). Since pK_a values of carboxyl groups are not expected to be dramatically affected by the increase in temperature, the pK_{a1} value (3.80) obtained by potentiometric titration at room temperature agrees fairly well with the value (3.97) obtained from the rate-pH profile.

Table 1
Calculated rate constants and pK_a values for the degradation of **I** and **II** at 80°C in accordance with Eqs. (3) and (4), respectively

I		**II**	
k_H (h^{-1} M^{-1})	1.92 (±0.04)	k_H (h^{-1} M^{-1})	2.33 (±0.04)×10^{-1}
k_o (h^{-1})	2.41 (±0.05)×10^{-2}	k_o (h)	5.12 (±0.10)×10^{-2}
k'_o (h^{-1})	1.79 (±0.04)×10^{-3}	k'_o (h^{-1})	8.13 (±0.15)×10^{-2}
k'_{OH} (h^{-1} M^{-1})	69.2 (±1.7)	k''_o (h^{-1})	1.05 (±0.02)×10^{-3}
pK_{a1}	3.97 (±0.06)	pK_{a1}	2.82 (±0.08)
		pK_{a2}	4.37 (±0.09)

3.3. Degradation in strongly acidic solutions

Under highly acidic conditions (pH < 2), the three amide bonds are the potential hydronium-ion-catalyzed hydrolysis sites (Scheme 1). The hydrolysis of the side-chain amide bond of **I** forming **II** constitutes the major degradation route. Klerval (**I**) and the hydrolysis product (**II**) undergo further fragmentation to yield the tripeptide (**III**) and dipeptide (**IV**). The detection of a very small amount of the succinimide (**V** in Scheme 2) at the pH range of 1–2 represents a minor degradation pathway. This is illustrated by the results obtained at pH 1.1 (Fig. 3a), where approximately 78% of **I** underwent side-chain deamidation generating **II**; 18% direct cleavage of the aspartyl peptide bond yielding **III**; and only 2% cyclization forming **V.** The computer-generated rate-pH profiles for the formation of various degradation products are shown in Fig. 4.

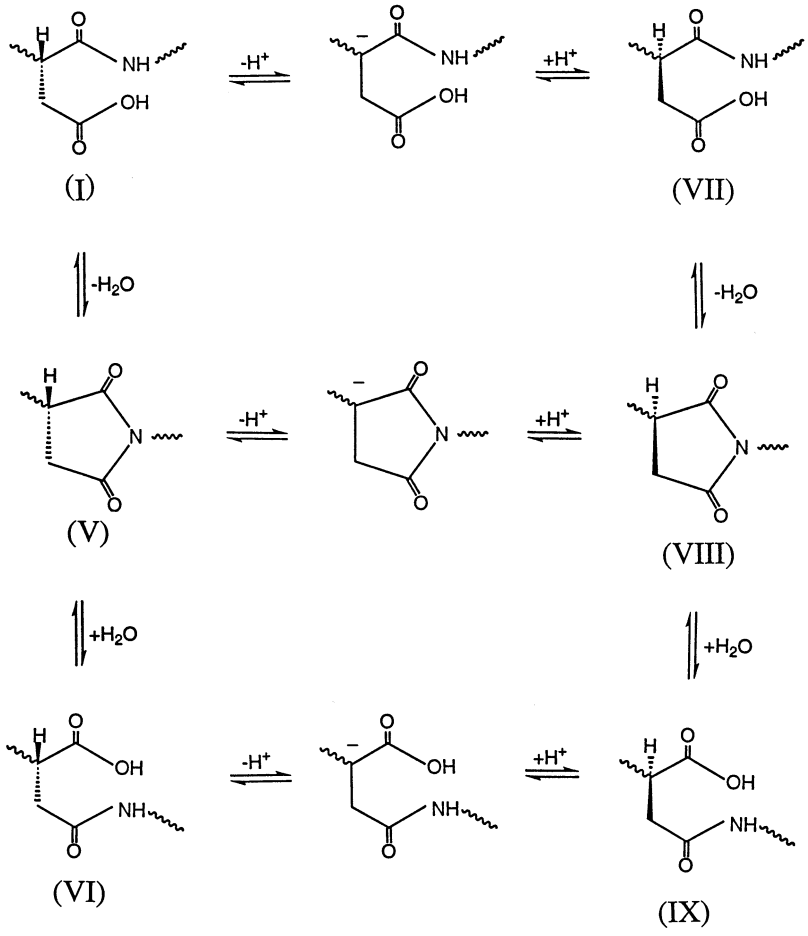

Scheme 2.

3.4. Degradation in weakly acidic solutions

The degradation pathway involving direct hydrolysis of the amide side-chain to generate **II** is an acid-catalyzed process, and the route yielding **III** is a pH-independent reaction between pH 1 and 3. Therefore, as pH increases under weakly acidic conditions ($2 < pH < 5$), the rate of **II** formation decreases significantly and the formation of **III** becomes predominant (Fig. 3b). The degradation route forming the succinimide (**V**) also becomes progressively noticeable as the overall degradation rate decreases. The succinimide (**V**), which is stable under strongly acidic conditions, degrades further to form **VI** in weakly acidic solutions. At pH 4.0, it was observed that 73% of **I** degraded via the pathway leading to **III** and 27% to **V** (Fig. 3b). The deamidation rate for **I** was slow enough that an insignificant amount ($< 1\%$) of **II** was formed.

The relative maximum concentration of the succinimide intermediate (**V**) was found to be low ($< 10\%$) and the low concentration did not allow the rate constants for the formation and decomposition of **V** to be determined with suitable precision. The pH dependence of the computer-generated rate constants for the formation of **V** appears to be sigmoidal (Fig. 4). As the observed apparent pattern is within the amount of fluctuation that can be attributed to systematic fitting errors, no attempts were made to analyze the curve.

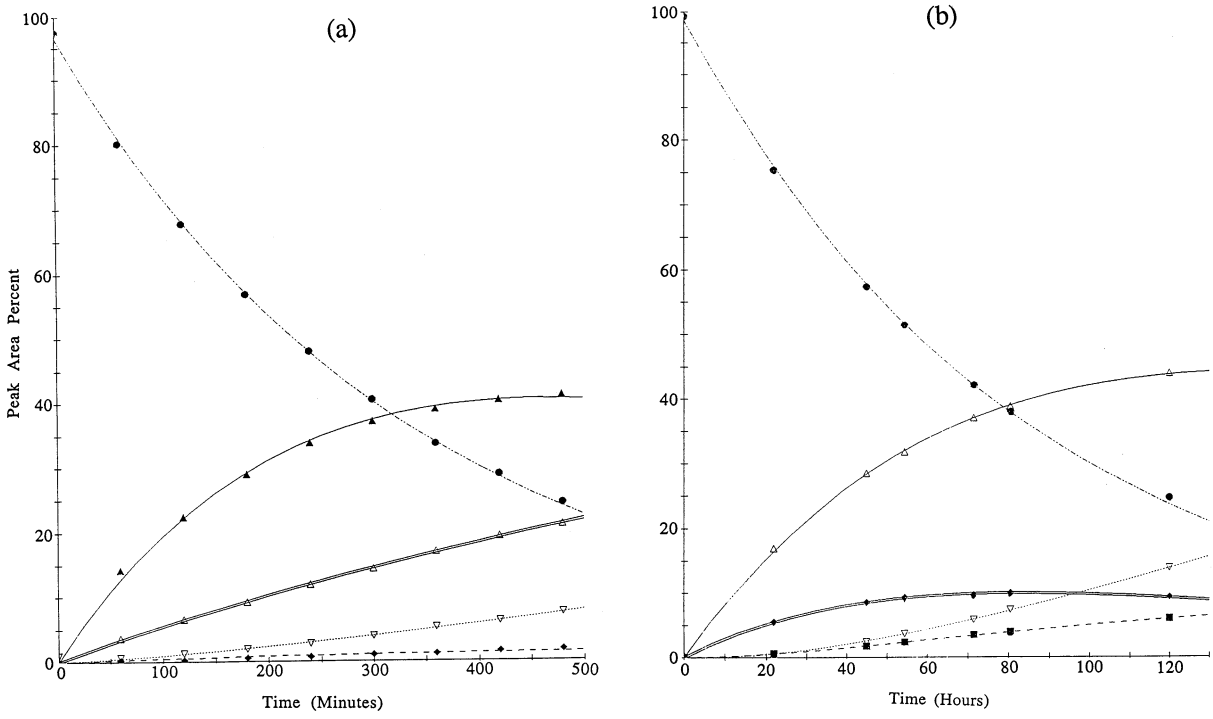

Fig. 3. (a) Time course for **I** (●), **II** (▲), **III** (△), **IV** (▽), and **V** (◆) during the degradation of **I** in 0.1 N HCl at 80°C. (b) Time course for **I** (●), **III** (△), **IV** (▽), **V** (◆), and **VI** (■) during the degradation of **I** in acetate buffer of pH 4.0 at 80°C. Both L- and D-epimers are included in **V** and **VI**.

The shape of the rate-pH profile for the formation of **III** is shown in Fig. 4. The variation of the rate constant from pH 1 to 5 indicates kinetic rate dependence on the degree of the undissociated carboxyl form of the aspartyl residue and independence of the external hydronium-ion concentration. This pH dependence is characterized by consistency of the rate constant from pH 1 to 3 and a decrease in the rate constant from pH 3 to 5 as the carboxyl group ionizes.

Aspartyl-peptide bonds are known to be selectively hydrolyzed under mildly acidic conditions (Marcus, 1985). A mechanism of neighboring carboxyl-group catalysis in the hydrolysis of the amide bond of **I** forming **III,** which accommodates the kinetic data, is an intramolecular nucleophilic displacement of the protonated amide by carboxylate anion of the aspartyl residue as shown in Scheme 3 (Piszkiewicz et al., 1970). Since NH_2 is a poor leaving group, protonation of the leaving group is of primary importance for the hydrolysis of the amide bond. Only unionized neighboring carboxyl group is able to protonate NH_2 and catalyze the hydrolysis (Thanassi and Bruice, 1966). As pH increases beyond 4, the concentration of the undissociated carboxyl group decreases and, hence, the intramolecular carboxyl-group catalysis decreases.

The degradation of **II**, which has two carboxyl groups, proceeds approximately 3 times as fast as that of **I** in the pH range of 3–4 (Fig. 2). The rate-pH profile for the degradation of **II** demonstrates a bell-shaped curve with the maximum rate between two pK_a values (2.8 and 4.4) of the carboxyl groups. The rate maximum is approximately at the pH corresponding to the maximum concentration of the singly-ionized species.

The observed rate constant for the degradation of **II** excluding the alkaline region can be formulated as shown in Eq. (4).

$$k_{obs} = (k_H[H^+] + k_o)f_c + k'_o f_z + k''_o f_a$$
$$= \{(k_H[H^+] + k_o)[H^+]^2 + k'_o K_{a1}[H^+]$$
$$+ k''_o K_{a1}K_{a2}\}/([H^+]^2 + K_{a1}[H^+] + K_{a1}K_{a2}) \quad (4)$$

where f_c, f_z and f_a are fractions of cation, zwitterion and anion, respectively, and k_H, k_o, k'_o and k''_o are rate constants corresponding to hydronium-ion-catalyzed reaction of the cation, solvent catalyzed reactions of the zwitterion and the anion or their kinetic equivalents, respectively. The values (Table 1) for the rate constants and ionization constants were estimated from the nonlinear regression of the plots of the observed rate of degradation of **II** versus pH in Fig. 2.

The acceleration of the rate and the bell-shaped profile can be explained by an intramolecular bifunctional catalysis (Morawetz and Oreskes, 1958; Morawetz and Shafer, 1962) in which suitably spaced two carboxyl groups (a carboxyl group and a carboxylate anion) participate in hydrolysis (Scheme 3). The C-terminal carboxylate anion attacks the carbonyl carbon while the unionized side-chain carboxyl group of the aspartic acid stabilizes the 6-membered-ring transition state by hydrogen bonding to the leaving group.

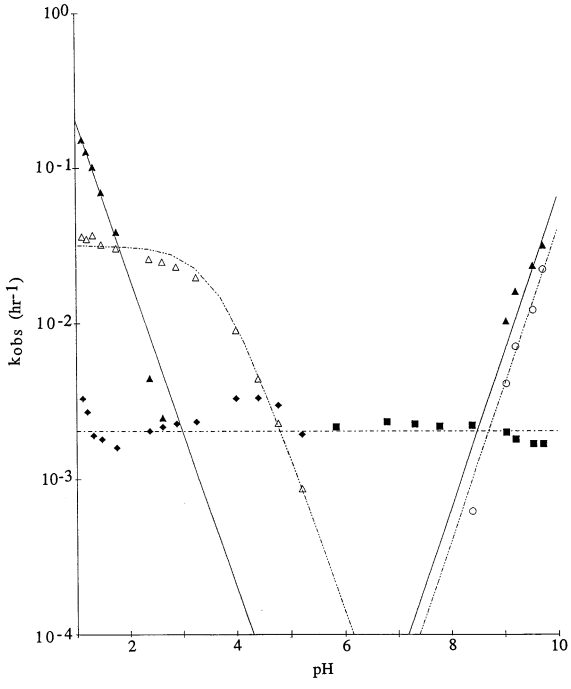

Fig. 4. The rate-pH profiles for the formation of **II** (▲), **III** (△), **V** (◆), **VI** (■), and **VII** (○) in the degradation of **I** at 80°C. Both L- and d-epimers are included in **V** and **VI**.

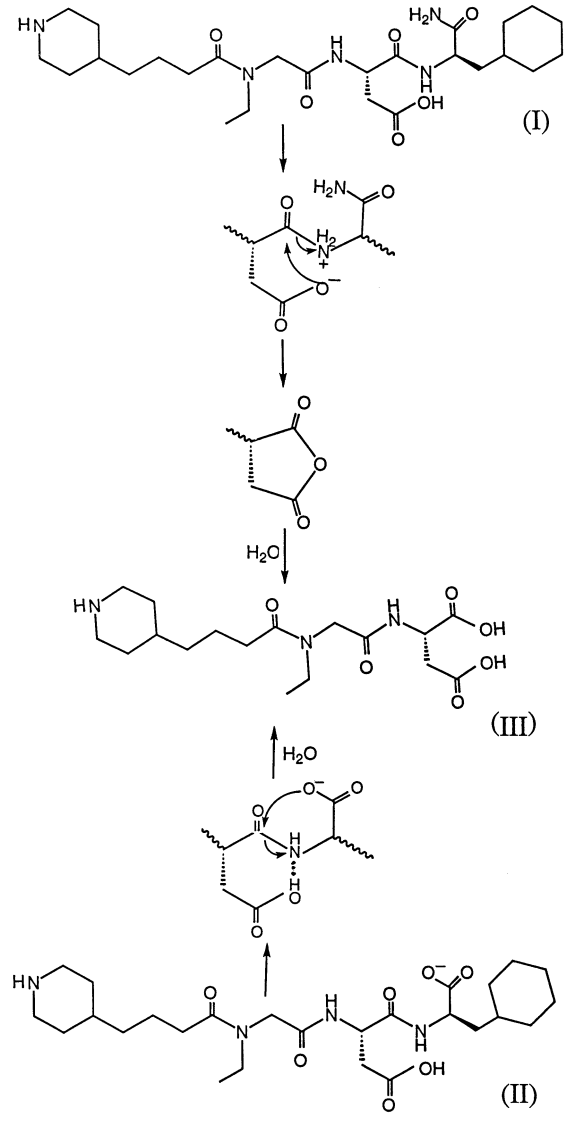

Scheme 3.

3.5. Degradation in neutral-to-basic solutions

At neutral pH ($5 < pH < 8$), the acid- or base-catalyzed hydrolysis is negligible and the domi-

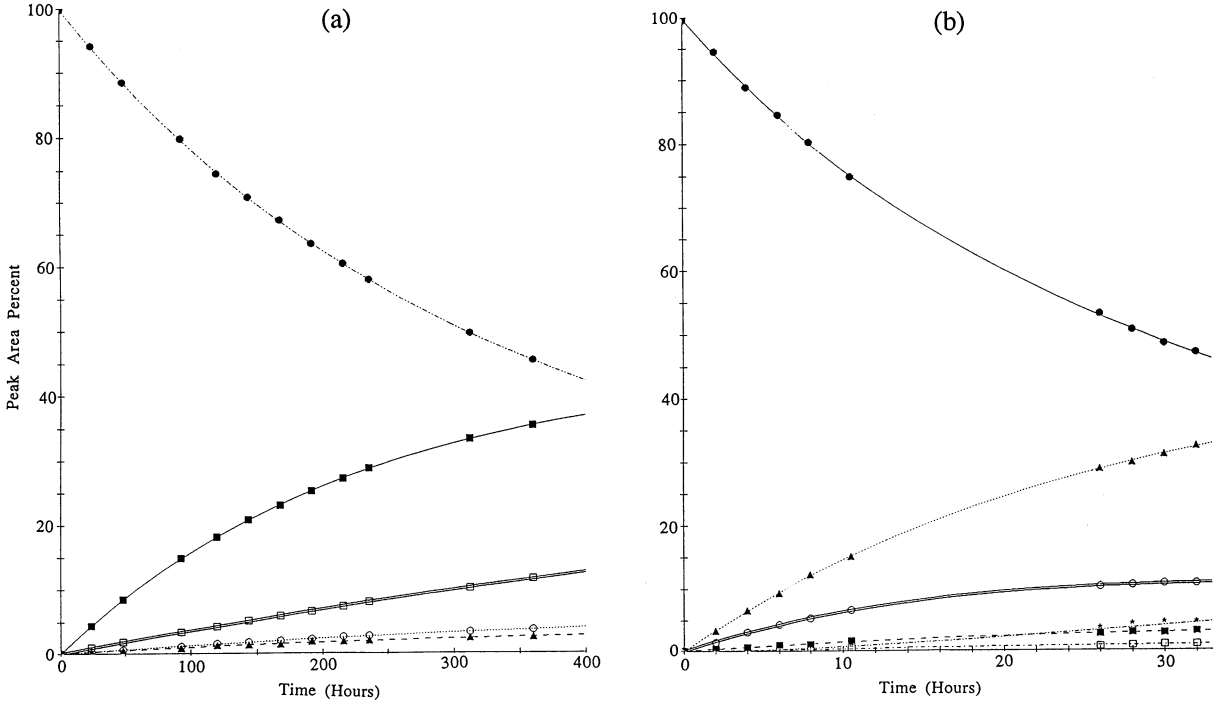

Fig. 5. (a) Time course for **I** (●), **II** (▲), **VI** (■), **VII** (○) and **IX** (□) during the degradation of **I** in phosphate buffer of pH 7.0 at 80°C. (b) Time course for **I** (●), **II** (▲), **VI** (■), **VII** (○), **IX** (□) and D-epimer of **II** (*) in the degradation of **I** in carbonate buffer of pH 9.3 at 80°C.

nant reaction is isomerization leading to the formation of the isoaspartyl peptide **VI** (Fig. 5a). The formation of **VI** can only be explained by a mechanism involving conversion of the backbone amide to the succinimide (**V**) and subsequent hydrolysis to a mixture of normal (**I**) and isoaspartyl (**VI**) forms (Scheme 2). The formation of **V** from **I** entails an intramolecular cyclization involving a nucleophilic attack of the aspartyl side-chain carbonyl carbon by the peptide-bond nitrogen and subsequent loss of the hydroxyl moiety to form a succinimidyl residue. As pH of the solution increases above 5 where **I** exists as a zwitterion, the cyclization rate is expected to be independent of pH reflecting the rate of water-catalyzed reaction of the zwitterion. As the carboxylate oxygen is unprotonated in this pH region and thus is a very poor leaving group, the formation of the succinimide from the zwitterion is expected to be a slow process.

In general, succinimides are stable in acidic solutions, but the stability progressively diminishes with increasing pH (Yakatan and Fan, 1977). The hydrolysis of L-succinimide (**V**) and D-succinimide (**VIII**) at 80°C went to completion instantaneously at pH 9.3 and within an hour at pH 7.0. The D-succinimide ($k = 0.252\ h^{-1}$ at pH 7.0, 50°C) demonstrated increased stability relative to the L-succinimide ($k = 0.452\ h^{-1}$ at pH 7.0, 50°C). This is consistent with previous observations in an ACTH hexapeptide (Geiger and Clarke, 1987) and tetragastrin (McFadden and Clarke, 1986).

As the hydrolysis of the succinimide ring becomes much faster than its formation with increasing pH, the succinimide intermediate (**V**) is no longer detectable. The formation of the succinimide intermediate may be the rate-determining step of the pH-independent isomerization reaction.

In alkaline pH region (pH > 8), rapid deamidation of the side-chain amide group of **I** to **II** is again apparent, but the epimerization of **I**–**VII** is rapid enough to compete with the deamidation reaction (Fig. 5b). At pH 9.3, 64% of **I** underwent hydrolysis to **II**, 30% epimerization to **VII** (28%) and **IX** (2%), and 6% isomerization to **VI**. The deamidation and epimerization reactions are specific hydroxyl-ion catalyzed.

The epimerization of L-succinimide (**V**), resulting in the formation of D-normal (**VII**) and D-iso (**IX**) peptides competes with the hydrolysis to L-normal (**I**) and L-iso (**VI**) peptides. The epimerization and hydrolysis of the succinimides are reversible reactions and represent progress toward an equilibration of **I**, **VI**, **VII** and **IX**. The equilibrium concentrations of the products at pH 7.0 and 9.3 are given in Table 2. The data suggest that the hydrolysis products are favored to epimerization products. It is noteworthy that thermodynamic equilibrium favors isopeptides over normal peptides in the hydrolysis of the succinimides. The preferential isopeptide formation from succinimdes has also been observed for the succinimides of an ACTH hexapeptide (Geiger and Clarke, 1987) and daptomycin (Kirsch et al., 1989).

Table 2
Equilibrium concentrations (%) in the hydrolysis of **V** and **VIII** and rate percent for the interconversion of **I**, **VI** and **VII** at 80°C[a]

pH	Reactant	Products			
		I	**VI**	**VII**	**IX**
7.0	**V**	17.5	64.2	3.0	15.3
	VIII	9.6	19.1	11.4	59.9
	I	–	72.5	5.9	17.0
		(74.2)	(3.5)	(17.7)	
	VI	44.7	–	5.3	41.3
		(44.6)		(7.7)	(39.0)
	VII	13.1	18.6	–	59.7
		(10.3)	(19.5)		(61.6)
9.3	**V**	19.5	67.8	1.9	10.8
	VIII	8.6	14.4	11.5	65.5
	I	–	6.4	28.3	1.5
			(30.5)	(0.8)	(4.9)
			[6.8]	[28.3]	[1.1]
	VI	2.4	–	<1	18.0
		(12.4)		(1.2)	(6.8)
		[5.6]		[0.5]	[14.3]
	VII	31.7	<1	–	4.4
		(3.5)	(5.9)		(26.7)
		[29.0]	[1.3]		[5.8]

[a] The percent values in ( ) were calculated assuming the reaction went through the succcinimde intermediates. The percent values in [ ] were calculated assuming 99.3% of the epimerization of **I**, 78.4% of **VI** and 97.2% of **VII** were direct and the rest were indirect through the succinimides.

The formation rate constants of various degradation products in the degradation of **I** at pH 7.0 (Fig. 5a) and pH 9.3 (Fig. 5b) were estimated by an initial-rate method (Jencks, 1987). Similar rate measurements were carried out with **VI** and **VII** degradation. The rate percent for each isomerization and epimerization pathway is listed in Table 2. Assuming the interconversion of the peptides occurs only via the succinimide intermediates (**V** and **VIII**), the percent rate for each pathway was calculated. The results demonstrate that practically total conversion can be attributed to the succinimide intermediates at pH 7.0.

The mechanism for the epimerization of peptides involves removal of an α-proton by a base to form a carbanion intermediate. The stability of the carbanion intermediate depends on the inductive and resonance effects of the α-carbon substituents. The carboxylate anion has been found to have negative influence on the epimerization rate through its direct field effect on the incipient carbanion (Smith and Baum, 1987). It has been found that removal of the carboxylate anion by ester or amide formation enhances racemization (Matsuo et al., 1967). In addition, increased resonance of the carbanion of succinimides through two carbonyl groups is expected to stabilize the carbanion and, hence, enhance the racemization rate of the cyclic imides. Although succinimides are unstable and present in only trace quantities, cyclization of aspartyl peptides to succinimides and the subsequent epimerization is likely to be the principal epimerization pathway at neutral pH (Geiger and Clarke, 1987).

Base catalysis of the epimerization is indicated by the increase in epimerization rates with increasing pH (Fig. 4). If the succinimides (**V** and **VIII**) were the only species that undergo epimerization and no epimerization of other species occur, the ratio of the formation rates of **VII**–**IX** should be irrelevant to the starting peptide, **I** or

VI. The fact that **VII**, **IX** or **I** is a major product in the degradation of **I**, **VI** or **VII**, respectively, indicates the direct epimerization at the aspartyl and isoaspartyl peptides. The rates of the peptide epimerization determined at pH 9.3 are much faster than that predicted assuming the succinimides are the only epimerizing species (Table 2). The calculated interconversion rates agree fairly well with observed rates when 99.3% of the epimerization of **I**, 78.4% of **VI** and 97.2% of **VII** are assumed to occur directly and the rest via the succinimides. In other words, more direct epimerization occurs in the normal peptide than the isopeptide as the carbanion of the normal peptide is probably more stable than that of the isopeptide.

As pH increases further, the rate of the pH-independent formation of the succinimide from the peptides becomes slow relative to its pH-dependent decomposition reactions. Accordingly, the contribution to the total epimerization rate via the succinimides becomes less significant with increasing pH.

Acknowledgements

The authors thank Dr B. Hsu for mass spectral analysis, Dr M. Vuilhorgne for NMR analysis and Dr B. Vanasse for helpful discussions in the preparation of degradation products.

References

Geiger, T., Clarke, S., 1987. Deamidation, isomerization and racemization at asparaginyl and aspartyl residues in peptides. J. Biol. Chem. 262, 785–794.

Harned, H.S., Owen, B.B., 1958. The Physical Chemistry of Electrolyte Solutions. Rheinhold, New York, p. 176.

Jencks, W.P., 1987. Catalysis in Chemistry and Enzymology. Dover, New York, p. 565.

Kirsch, L.E., Molloy, R.M., Debono, M., Barker, P., Farid, K.Z., 1989. Kinetics of the aspartyl transpeptidation of daptomycin, a novel lipopeptide antibiotic. Pharm. Res. 6, 387–393.

Marcus, F., 1985. Preferential cleavage at aspartyl-prolyl peptide bonds in dilute acid. Int. J. Protein Res. 25, 542–546.

Matsuo, H., Kawazoe, Y., Sato, M., Ohnishi, M., Tatsuno, T., 1967. Studies on the racemization of amino acids and their derivatives. I. On the deuterium-hydrogen exchange reaction of amino acid derivatives in basic media. Chem. Pharm. Bull. 15, 391–398.

McFadden, P.N., Clarke, S., 1986. Chemical conversion of aspartyl peptides to isoaspartyl peptides. J. Biol. Chem. 261, 11503–11511.

Morawetz, H., Oreskes, I., 1958. Intramolecular bifunctional catalysis of ester hydrolysis. J. Am. Chem. Soc. 80, 2591–2592.

Morawetz, H., Shafer, J., 1962. Intramolecular bifunctional catalysis of amide hydrolysis. J. Am. Chem. Soc. 84, 783–3784.

Oliyai, C., Borchardt, R.T., 1993. Chemical pathways of peptide degradation. IV. Pathways, kinetics, and mechanism of degradation of an aspartyl residue in a model hexapeptide. Pharm. Res. 10, 95–102.

Piszkiewicz, D., Landon, M., Smith, E.L., 1970. Anomalous cleavage of aspartyl-proline peptide bonds during amino acid sequence determinations. Biochem. Biophys. Res. Comm. 40, 1173–1178.

Pytela, R., Pierschbacher, M.D., Ginsberg, M.H., Plow, E.F., Ruoslahti, E., 1986. Plate membrane glycoprotein IIb/IIIa: member of a family of arg-gly-asp-specific adhesion receptors. Science 231, 1559–1562.

Smith, G.G., Baum, R., 1987. First-order rate constants for the racemization of each component in a mixture of isomeric dipeptides and their diketopiperazines. J. Org. Chem. 52, 2248–2255.

Stephenson, R.C., Clarke, S., 1989. Succinimde formation from aspartyl and asparaginyl peptides as a model for spontaneous degradation of proteins. J. Biol. Chem. 264, 6164–6170.

Thanassi, J.W., Bruice, T.C., 1966. Neighboring carboxyl group participation in the hydrolysis of monoesters of phthalic acid. The dependence of mechanisms on leaving group tendencies. J. Am. Chem. Soc. 88, 747–752.

Tsuda, T., Uchiyama, M., Sato, T., Yoshino, H., Tsuchiya, Y., Ishikawa, S., Ohmae, M., Watanabe, S., Miyake, Y., 1990. Mechanism and kinetics of secretin degradation in aqueous solutions. J. Pharm. Sci. 79, 223–227.

Yakatan, G.J., Fan, T., 1977. Kinetics of hydrolysis of succinimides. Drug Dev. Ind. Pharm. 3, 315–338.